

THz BURSTING THRESHOLDS MEASURED AT THE METROLOGY LIGHT SOURCE

M. Ries*, J. Feikes, P. Schmid, G. Wüstefeld, Helmholtz-Zentrum Berlin, Germany
A. Hoehl, Physikalisch-Technische Bundesanstalt, Berlin, Germany

Abstract

At the Metrology Light Source (MLS) [1] owned by the Physikalisch-Technische Bundesanstalt (PTB) the bunch length can be varied by more than two orders of magnitude [2]. The bunch length manipulation is achieved by varying different machine parameters, such as RF-voltage amplitude up to 500 kV and the momentum compaction factor α over three orders of magnitude. The subject of this article is the measurement of THz bursting thresholds at the MLS for different bunch lengths.

INTRODUCTION

Short bunch operation of electron storage rings is motivated by users interested in short photon pulses as well as the generation of coherent synchrotron radiation (CSR). The bunch current that is stably storable in short bunches is limited by various storage ring parameters. The transition from stable to bursting CSR was first observed at BESSY II [3]. The transition point is called bursting threshold and was measured at several light sources by now. The value of the threshold depends on various properties e.g. beam optics, RF-parameters and the dimensions of the vacuum chamber. Understanding the bursting process is relevant for the design of new short pulse storage rings [4] or other high peak current facilities.

STORAGE RING PREPARATION

The first three orders of the momentum compaction factor $\alpha(\delta) = \alpha_0 + \alpha_1\delta + \alpha_2\delta^2 \dots$ as a function of the momentum deviation $\delta = \frac{\Delta p}{p_0}$ were set to the desired values [2]. α_0 was directly measured by Compton backscattering to check the scaling of the synchrotron oscillation frequency f_s with RF-voltage V . A measurement of the longitudinal tune was then used to calculate α_0 . The higher orders α_1 and α_2 were adjusted as close to zero as possible by dedicated sets of sextupole and octupole magnets eliminating the RF-frequency dependence of the longitudinal tune. Transverse chromaticities were set to small positive values (≈ 0.2). Individually powered quadrupoles were used to eliminate the dispersion D and its derivative D' at the position of the RF-cavity avoiding transverse-longitudinal coupling predicted by tracking simulations. The current measurement was performed with a diode calibrated by a current transformer. Single bunch operation was chosen to avoid ion effects, coupled bunch instabilities and filling pattern inhomogeneities.

* markus.ries@helmholtz-berlin.de

Table 1: Selected MLS Machine Parameters

parameter	value
electron energy	≤ 629 MeV
α_0	$-3 \cdot 10^{-2}$ to $7 \cdot 10^{-2}$
circumference	48 m
RF-frequency f_{RF}	500 MHz
RF-voltage V	≤ 500 kV
dipole bending radius ρ	1.528 m
full vacuum chamber height h	42 mm

THz BURSTING

Measurement Setup

Bursting measurements were carried out at the THz beam port of the MLS [5]. As a detector an InSb hot electron bolometer was used. Its spectral sensitivity ranges up to 50 cm^{-1} . The detector is only able to resolve frequencies of up to 1 MHz and therefore unable to resolve the revolution time of a single bunch. However, it is fast enough to measure fluctuations of the CSR power introduced by bursting, expected to be below 200 kHz. The InSb signal was recorded using a spectrum analyzer.

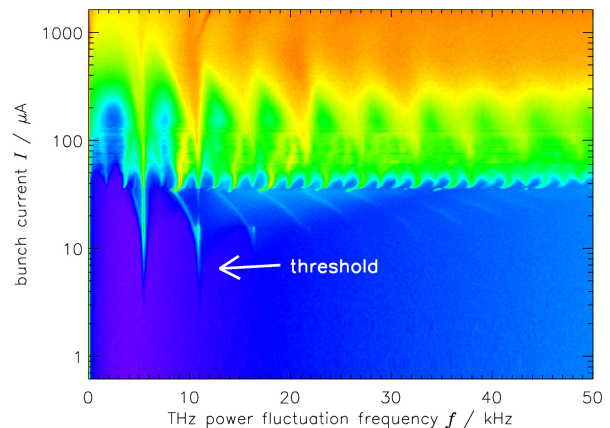


Figure 1: Temporal fluctuation of the THz power as a function of the single bunch current plotted in the frequency domain. The measurement was performed using an InSb hot electron bolometer at a the storage ring parameters $\alpha_0 = 1.3 \cdot 10^{-4}$ and $V = 330$ kV.

Measurement

All measurements discussed here were conducted at an electron beam energy of 629 MeV. Figure 1 shows a measurement where the electron current was changed

by about three orders of magnitude with other parameters fixed. Bursting starts at about $5 \mu\text{A}$. The variation of the RF-voltage is another way to find the bursting threshold. Thus multiple bursting thresholds can be measured without changing the magnetic properties of the storage ring. For a given beam optics (α) and single bunch current I the RF-voltage was slowly changed. Measurements show that there is no significant difference whether V is increased or decreased to determine the threshold. The threshold does not differ between entering or leaving the bursting regime. Figure 2 shows a selected measurement of a bursting threshold using the variation of the RF-voltage. The different appearance compared to Fig. 1 is caused by a different parameter range in terms of I , U and α_0 .

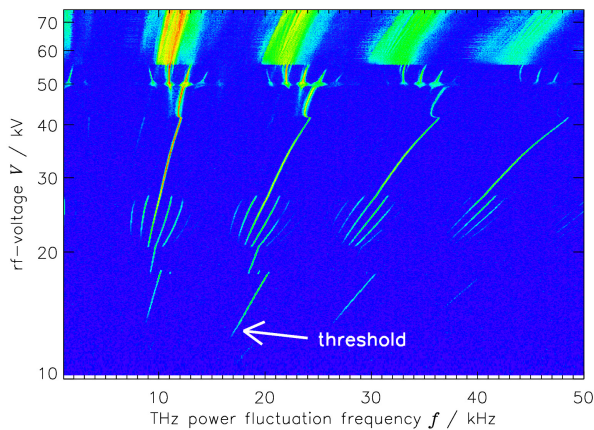


Figure 2: Temporal fluctuation of the THz power as a function of RF-voltage in the frequency domain. The measurement was performed at the storage ring parameters $\alpha_0 = 5 \cdot 10^{-4}$ and $I = 300 \mu\text{A}$.

Periodic fluctuations of the CSR power at the onset of the instability are observed at characteristic frequencies in the range up to 50 kHz depending on I , α_0 and V . As a criterion for the experimental identification of the bursting threshold a signal of 10 dB above the noise floor was chosen. This value compromises between an overestimation of the threshold and the measurement error and has proven to yield consistent results. The drawback of this definition is that it means the bunch is already bursting. Figure 3 shows a set of spectra near the threshold according to the previous definition.

The MLS control system [6] allowed to fully automate measurements resulting in a high resolution and high reproducibility. The algorithm can be outlined as:

1. sweep RF-voltage slowly e.g. from 500 kV to 15 kV,
2. during sweep:
 - record Fourier transform of THz bursting signal
 - record other beam parameters
3. at the end of sweep:
 - restore RF-voltage

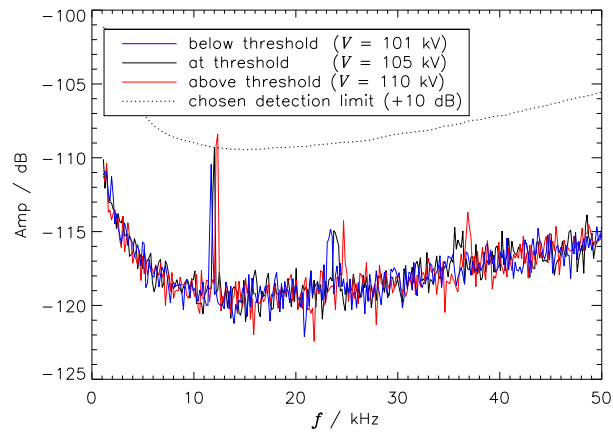


Figure 3: RF-voltage dependence of the THz power at the bursting threshold. The black line shows the spectrum of the fluctuations of the CSR power measured by an InSb hot electron bolometer. Blue and red lines indicate the spectra below and above the threshold.

- use automatic scraper procedure to reduce current e.g. by 5%

4. repeat.

Offline analysis yields one value for the bursting threshold per sweep.

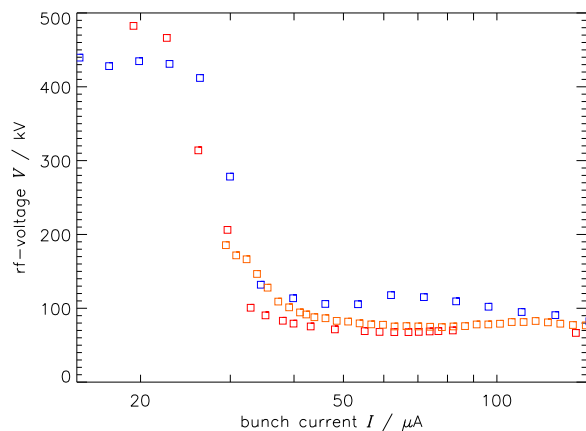


Figure 4: Examples of bursting threshold measurements at 629 MeV with $\alpha_0 = 0.0005$. One bursting threshold (one data point) corresponds to one RF-voltage sweep as shown in Fig. 2.

Figure 4 shows sets of measurements of the current dependent bursting threshold at one specific α_0 . A very characteristic feature is a steep change in the voltage needed to reach the bursting threshold in the range from $20 \mu\text{A}$ to $30 \mu\text{A}$ single bunch current. This feature is found for different α_0 at different RF-voltages, but always at zero-current bunch lengths in the range from 0.8 mm to 1.6 mm.

Scaling Laws

Measurements were repeated to check for reproducibility as well as different influences e.g. octupole. Figure 5

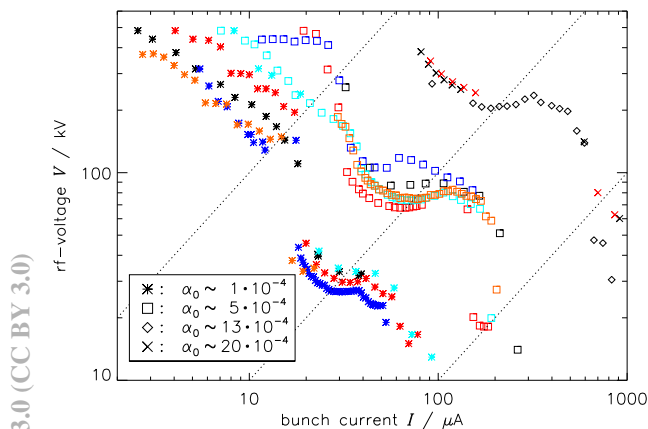


Figure 5: Results of the measurement of the bursting threshold. Different symbols correspond to different α_0 . Colors indicate measurement sets within one α_0 set. Dotted lines correspond to $I/V = \text{constant}$.

shows multiple sets of measurements for different α_0 . One measurement (cyan box) was taken at a large value of α_2 (≈ 10), which seems to have an influence in the short bunch length regime. All measurements show the same structure implying that there is a scaling law involved allowing to plot the results in scaled units.

The calculation of bursting thresholds can be approached from coasting beam theory as well as from the bunched beam theory [7, 8]. Both theories yield results, which can be written in the following form:

$$\sigma^{\frac{7}{3}} = \frac{Z_0 c^2 q \rho^{\frac{1}{3}}}{8\pi^2 \xi^{\text{th}} f_{\text{RF}}^2} \frac{I}{V \cos(\phi_s)}, \quad (1)$$

whereas σ is the bunch length, Z_0 the free space impedance, q the harmonic number and ϕ_s the synchronous phase. For bunched beam theory the scaled threshold current ξ^{th} can be approximated by:

$$\xi^{\text{th}} = \xi^{\text{th}}(\chi) = 0.5 + 0.34\chi - 0.385e^{-\frac{(\chi-0.25)^2}{2 \cdot 0.02^2}}, \quad (2)$$

with the shielding parameter $\chi = \sigma \rho^{\frac{1}{2}} / h^{\frac{3}{2}}$. $\xi^{\text{th}}(\chi)$ is extracted from [8] and additionally modified by a Gaussian dip to roughly account for a drop of the expected threshold at $\chi = 0.25$ [7]. From coasting beam theory follows:

$$\xi^{\text{th}} = 7.456 \cdot 3^{\frac{1}{3}} / 4\pi \approx 0.856. \quad (3)$$

Taking into account the MLS machine parameters from Tab. 1, the dip of Eq. 2 generated by the Gaussian is situated at a bunch length of $\sigma_{\text{dip}} = 1.7 \text{ mm}$ (5.8 ps). Figure 6 corresponds to Fig. 5 but uses a scaled view in analogy to Eq. 1 to account for different machine parameters [9]. The bunch length was not measured. Instead the zero current

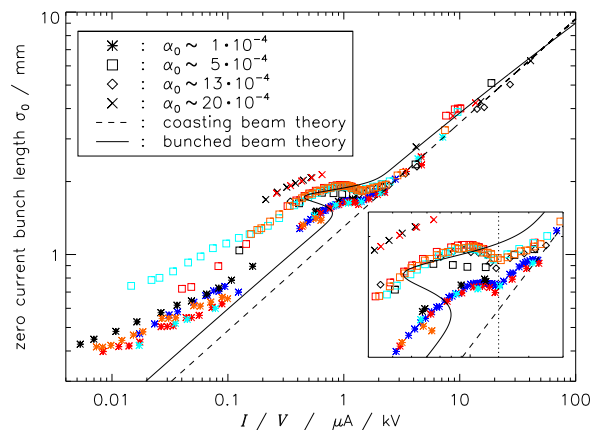


Figure 6: Scaled values of measured bursting thresholds. Different symbols correspond to different α_0 . Colors indicate measurement series within one α_0 set. The small inset is a zoom in the region, where the sets start to spread. The dotted line marks $I/V = 1.4 \mu\text{A}/\text{kV}$.

bunch length σ_0 was calculated based on measuring V and f_s [8]. The bunch lengths obtained agree well compared with streak camera measurements for larger bunch lengths. The scaling agrees with the theory for bunch lengths larger than 2 mm. At about σ_{dip} there is a characteristic feature in the data (cf. Fig. 4,6). For smaller bunch lengths the measurements seem to systematically deviate from the scaling law in dependence of α_0 .

ACKNOWLEDGMENT

This work was excellently supported by our HZB and PTB colleagues in particular by R. Müller (PTB) and P. Kuske (HZB). It is a pleasure to thank C. Evain (former SOLEIL), V. Judin (ANKA) and I. Martin (DIAMOND) for very interesting cooperative measurements accompanied by very fruitful discussions. For ongoing support and comments we acknowledge the help of A. Jankowiak (HZB) and G. Ulm (PTB).

REFERENCES

- [1] B. Beckhoff et al., Phys. Status Solidi B 246, p. 1415 (2009).
- [2] J. Feikes et al., Phys. Rev. ST Accel. Beams 14, 030705 (2011).
- [3] M. Abo-Bakr et al., Phys. Rev. Lett. 88, 254801 (2002).
- [4] G. Wüstefeld et al., IPAC 2011, San Sebastián, Spain, p. 2936-2938 (2011).
- [5] R. Müller et al., J. Infrared Milli Terahz Waves 32, 742 (2011).
- [6] J. Feikes et al., IPAC 2011, San Sebastián, Spain, p. 2927-2929 (2011).
- [7] K. L. F. Bane, Y. Cai and G. Stupakov, Phys. Rev. ST Accel. Beams 13, 104402 (2010).
- [8] Y. Cai, IPAC 2011, San Sebastián, Spain, p. 3774 (2011).
- [9] G. Wüstefeld et al., IPAC 2010, Kyoto, Japan, p. 2508 (2010).